

Fluorescence Approach for Measuring Anthocyanins and Derived Pigments in Red Wine

Giovanni Agati,[†] Paolo Matteini,[†] Joana Oliveira,[§] Victor de Freitas,[§] and Nuno Mateus^{*,§}

[†]Institute of Applied Physics, National Research Council, Sesto Fiorentino (Florence), Italy

[§]Centro de Investigação em Química, Departamento de Química, Universidade do Porto, Porto, Portugal

ABSTRACT: A novel fluorescence approach to monitor the evolution of anthocyanins and derivatives in red wine was developed. Some red table wines and Port wine with different vintage years were first tested with the aim to determine the ideal fluorescent conditions. The fluorescence contribution of both monomeric and polymeric anthocyanins was studied by comparing their emission spectra. By measuring the F_{700}/F_{560} ratio on different wine samples and applying an inverted exponential function, it was possible to estimate the monomeric/polymeric anthocyanin absorbance ratio that is proportional to the relative content of the two classes of compounds. The methodology was further developed by using pure compounds representative of monomeric anthocyanins and anthocyanin–pyruvic acid adducts, namely, by using malvidin-3-*O*-glucoside and vitisin A. A fluorescence excitation ratio ($FER_{350/550}$) was considered for estimating the absorbance ratio between vitisin A and malvidin-3-*O*-glucoside. Overall, this work aims to use fluorescence to monitor the evolution of anthocyanin derivatives and to distinguish them from their anthocyanin precursors, thereby allowing the evolution of anthocyanin pigments during wine aging to be monitored, but it also may be useful to determine age markers or even geographical markers.

KEYWORDS: anthocyanin, fluorescence, vitisin A, red wine, pigments

■ INTRODUCTION

The color of red wine and its changes during wine storage and aging are associated with the chemical reactions involving anthocyanins. Anthocyanins are soluble pigments that are extracted from the red grape skins during maceration and fermentation.¹ These molecules are highly reactive and are readily involved in chemical reactions with other red wine components such as aldehydes or polyphenols (e.g., tannins), yielding new anthocyanin derivatives.^{2–10} Both anthocyanins and anthocyanin-derived pigments contribute to the color of young red wines and play a crucial role in color evolution during aging.

Among the different classes of anthocyanin derivatives formed during winemaking and aging, anthocyanin–pyruvic acid adducts appear to be the major class of compounds detected by HPLC after only 1 or 2 years of aging in Port wine.¹¹

A proper monitoring of anthocyanin pigments is critical because of the impact that some of these pigments may have on the overall color displayed by red wine. Such monitoring can be made in the grape skins during ripening (maturation control) or directly in red wine.¹² The methods employed usually rely on spectrophotometric assays or, more accurately, HPLC analysis.^{11,13} In the case of the analysis in grapes, those methods are destructive.

The nondestructive monitoring of anthocyanin compounds during the wine aging phase would represent a significant technological improvement in enology. Spectroscopic optical methods are well suited for this purpose, once the optical properties of the compounds to be monitored are known. Reflectance spectroscopy in the visible–NIR spectral range and colorimetry are largely employed to get information on the anthocyanin content and other parameters of wine, mainly

associated with chemometric analyses.¹⁴ Fluorescence spectroscopy of wine has been much less studied. It can add useful information on specific molecules and can be more sensitive than reflectance.

In general, anthocyanins are weakly fluorescent in solution (a fluorescence quantum yield of 4.1×10^{-3} for malvin was previously reported¹⁵), probably because of the efficient excited state proton transfer to water.¹⁶ However, aggregation or complexation to other molecules can induce a significant fluorescence of the resulting anthocyanin-derived compound.

Recently, the high excitation laser intensity of a confocal microscope allowed for the detection of anthocyanin red fluorescence, with excitation in the green, in anthocyanin-containing plant cells.¹⁷ In this way, anthocyanin fluorescence was used to study the anthocyanin intracellular transport in grapevine cells¹⁸ or to visualize the dynamics of the vacuole in red onion epidermal cells.¹⁹

Red fluorescence detected directly in red wine was also reported, but without explanation of the origin of this emission.²⁰

In this study, a fluorescence approach to monitor the evolution of anthocyanins and derivatives in red wine was attempted. First, some red table wine and Port wine samples were tested, and the technique was further developed by using pure compounds representative of anthocyanins and anthocyanin–pyruvic acid adducts, namely, by using malvidin 3-*O*-glucoside and vitisin A (Figure 1).

Received: May 31, 2013

Revised: September 20, 2013

Accepted: September 24, 2013

Published: September 24, 2013

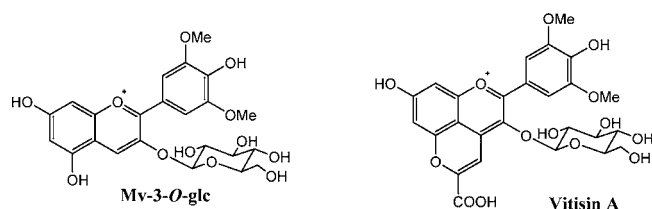


Figure 1. Chemical structures of malvidin 3-O-glucoside (Mv 3-O-glc) and malvidin 3-O-glucoside-pyruvic acid adduct (vitisin A).

MATERIALS AND METHODS

Wine Samples. The studied wines were four red Port wines from different vintage years (2009–2012) and two red table wines from two different vintage years (2011 and 2012) made from a mixed variety of grapes (*Vitis vinifera*) grown in the Douro Demarcated Region (northern Portugal): 2009 Port wine (alcohol 19.1% (v/v), pH 3.54, anthocyanins 18.6 mg/L, anthocyanin-pyruvic acid adducts 11.7 mg/L); 2010 Port wine (alcohol 19.43% (v/v), pH 3.50, anthocyanins 19.5 mg/L, anthocyanin-pyruvic acid adducts 16.1 mg/L); 2011 Port wine (alcohol 19.19% (v/v), pH 3.65, anthocyanins 101.1 mg/L, anthocyanin-pyruvic acid adducts 18.6 mg/L); 2012 Port wine (alcohol 18.63% (v/v), pH 3.70, anthocyanins 279.8 mg/L, anthocyanin-pyruvic acid adducts in trace amounts); 2011 table wine (alcohol 15.70% (v/v), pH 3.76, anthocyanins 504.2 mg/L, anthocyanin-pyruvic acid adducts in trace amounts); 2012 table wine (alcohol 14.68% (v/v), pH 3.80, anthocyanins 1362.2 mg/L, anthocyanin-pyruvic acid adducts in trace amounts).

Malvidin 3-O-Glucoside Isolation. Malvidin 3-O-glucoside was obtained from a grape skin extract according to what is reported elsewhere.^{21,22} The purity of malvidin 3-O-glucoside was confirmed by HPLC-DAD/MS and NMR.

Malvidin 3-O-Glucoside-Pyruvic Acid Adduct Synthesis and Purification. The synthesis of malvidin 3-O-glucoside-pyruvic acid adduct was obtained through the reaction of malvidin 3-O-glucoside with pyruvic acid according to the procedure described in the literature.²² The purity of the compound was assessed by HPLC-DAD/MS and NMR.

Isolation of Polymerized Anthocyanins. Polymerized anthocyanins were isolated from a 2-year-old red Port wine made from grapes of Touriga Nacional variety (*V. vinifera*) grown in the Douro Demarcated Region (northern Portugal) aged in bottle for 18 months [pH 3.5, 20% alcohol (v/v), total acidity 5.3 g/L, total SO₂ 22 mg/L]. The Port wine was fractionated by TSK Toyopearl HW-40(S) column chromatography using different aqueous solutions with increasing percentages of methanol up to 100% (v/v).²³ The obtained fractions were analyzed by HPLC-DAD/MS,²⁴ and the fraction containing the polymerized anthocyanins was the fraction obtained with 100% (v/v) methanol (data not shown).

Spectroscopic Measurements. Anthocyanins were directly dissolved either in an aqueous solution, containing 12% of ethanol, adjusted to pH around 1.0 by adding HCl, or in 0.1 M acetate buffer at pH 3.3 containing 12% of ethanol. At pH 1.0, only the flavylium cation form is known to be present. The pH 3.3 solution, containing 12% of ethanol, was used to simulate the acidic and alcoholic conditions usually found in wine.

Fluorescence (emission and excitation) spectra were measured by a Cary Eclipse spectrofluorometer [Agilent Technologies, Cernusco sul Naviglio (MI), Italy] in a 10 × 10 mm quartz cuvette, diluting the sample solutions to have an absorbance of about 0.1 in the 500–520 nm spectral region. Wine samples were diluted with the pH 3.3 solution. All fluorescence spectra were corrected for the spectral response of the spectrofluorometer emission and excitation units. Absorbance spectra were recorded by a Jasco model V-560 spectrophotometer (Jasco, Tokyo, Japan).

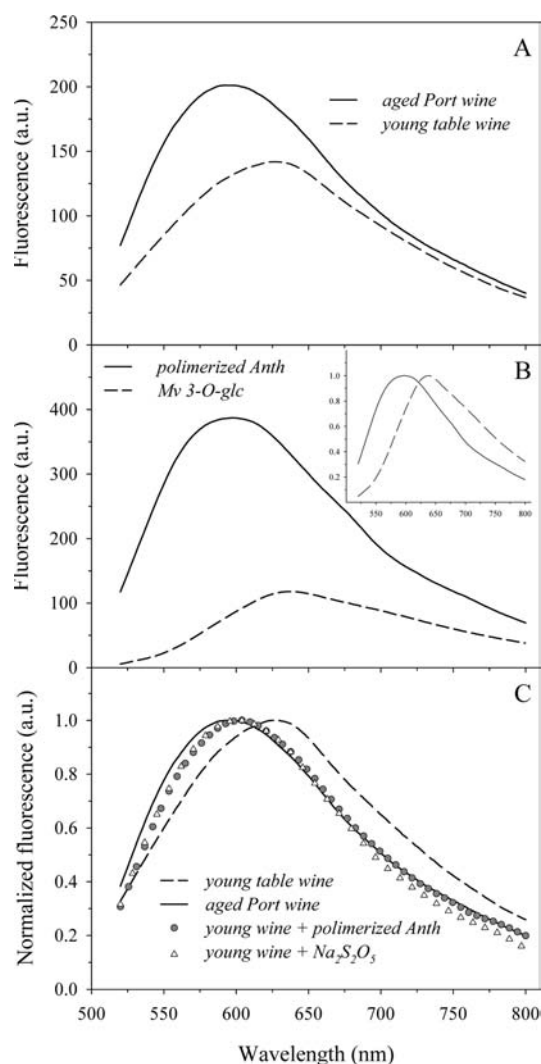


Figure 2. Fluorescence emission spectra for excitation at 500 nm of aged (2009) Port wine (solid line) and young (2012) table wine (dashed line) diluted with aqueous/EtOH solution at pH 3.3 (A); polymerized anthocyanins (solid) and malvidin 3-O-glucoside (Mv 3-O-glc, dashed) in aqueous/EtOH solution at pH 3.3, (inset) normalized spectra (B); normalized spectra of wines and young wine with the addition of polymerized Anth or treated with Na₂S₂O₅ (C). Emission spectra, average of three independent measurements, were corrected for differences in absorbance at 500 nm and smoothed.

RESULTS AND DISCUSSION

Fluorescence Features of Red Wine Samples. During aging, red wine anthocyanins undergo several chemical reactions yielding new anthocyanin derivatives that display different spectroscopic features resulting in color changes. Because anthocyanins are weakly fluorescent in solution, fluorescence spectroscopy of red wine has been poorly studied. Nevertheless, it can add useful information on specific molecules and can be more sensitive than reflectance as a result of aggregation or complexation to other molecules (including new derivatives) that can induce a significant fluorescence of the resulting anthocyanin-derived compound.

Therefore, the fluorescence band in the red spectral region of wines with different aging periods was assayed. The emission spectra of a 2012 young table red wine and a 3-year-old Port red wine, under excitation at 500 nm, are reported in Figure 2. The aged wine fluorescence peaked at about 595 and 30 nm

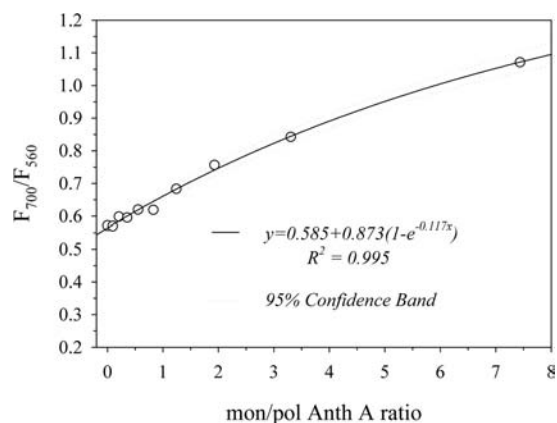


Figure 3. Relationship between the F_{700}/F_{560} fluorescence ratio and the absorbance ratio of monomeric and polymeric Anth compounds.

Table 1. F_{700}/F_{560} Ratio of Different Wine Samples and Resulting mon-/pol-Anth Absorbance Estimated by Applying the Exponential Function Determined in Figure 5

wine sample	F_{700}/F_{560}	mon-/pol-Anth absorbance
table wine 2012	0.99	5.75
table wine 2011	0.73	1.80
Port wine 2012	0.70	1.49
Port wine 2011	0.68	1.20
Port wine 2010	0.61	0.42
Port wine 2009	0.60	0.32
young wine	0.87	3.66
young wine + pol-Anth	0.64	0.74
young wine + $\text{Na}_2\text{S}_2\text{O}_5$	0.58	0.12

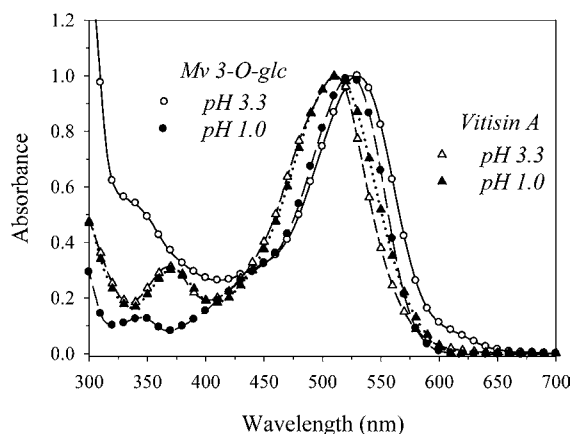


Figure 4. Absorption spectra of malvidin 3-O-glucoside (Mv 3-O-glc) and its pyruvic acid adduct (vitisin A) in aqueous/EtOH solution at pH 1.0 and 3.3. Spectra were normalized to their maximal absorbance in the green band.

shifted toward shorter wavelengths with respect to that of young wine (peak at 625 nm).

Aged wines usually contain larger amounts of polymerized anthocyanin (pol-Anth) pigments and lesser amounts of monomeric anthocyanin (mon-Anth) pigments compared to young wines.²⁵ It is likely that this different composition is reflected in the wine emission spectra.²⁶ Indeed, we found that the fluorescence band of pol-Anth isolated from wine and dissolved into the pH 3.3 ethanolic solution was quite similar (peak at 597 nm) to that of aged wines (Figure 2B). The pol-

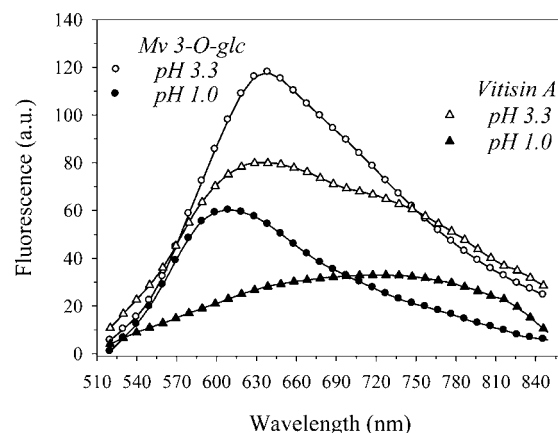


Figure 5. Fluorescence emission spectra of malvidin 3-O-glucoside (Mv 3-O-glc) and its pyruvic acid adduct (vitisin A) in aqueous/EtOH solution at pH 1.0 and 3.3. Emission spectra, the average of three to five independent measurements, were corrected for differences in absorbance at 500 nm and smoothed.

Anth fluorescence is much more intense than that of a solution of malvidin 3-glucoside (Mv 3-O-glc) at pH 3.3, used as standard for mon-Anth, as reported in Figure 2B for solutions at the same absorbance at 500 nm. The normalized spectra show a bathochromic shift of about 40 nm for mon-Anth with respect to pol-Anth (Figure 2B, inset).

When an aliquot of pol-Anth was added to the young wine sample, a hypsochromic effect was induced and the fluorescence spectral shape of the resulting mixture became similar to that of the aged wine (Figure 2C). Furthermore, treating the young wine with sulfur dioxide yielded again a shift of the fluorescence spectrum to shorter wavelengths to match the spectrum of old Port wine (Figure 2C). This is due to the formation of colorless and nonfluorescent compounds by the reaction between sulfur dioxide and mon-Anth.²⁷ In the case of pol-Anth, they remain unbleached because the physical site of sulfite binding is the same site engaged in the Anth polymerization.²⁸

Considering this, we can assume that the fluorescence band in the red spectral region of wines, under excitation at 500 nm, is due to the linear combination of the two main contributions from pol-Anth and mon-Anth pigments, as follows:

$$F^{500} = F_{\text{pol-Anth}}^{500} + F_{\text{mon-Anth}}^{500}$$

The fluorescence contribution of mon-Anth arises mainly from Mv 3-O-glc. Hence, by comparing the emission spectra of pol-Anth and Mv 3-O-glc (Figure 2B), it was observed that the large difference present at shorter wavelengths around 550–580 nm attenuated much when moving to longer wavelengths. Therefore, it may be assumed that a fluorescence ratio between these two spectral regions could be sensitive to changes in the relative content of pol-Anth and mon-Anth compound classes.

To prove this, two aqueous solutions of pol-Anth and Mv 3-O-glc were combined in different proportions, and the fluorescence spectra of the mixtures were analyzed. The fluorescence ratio F_{700}/F_{560} between emission around 700 and 560 nm under excitation at 500 nm were plotted against the absorbance ratio of Mv 3-O-glc and polymeric Anth compounds (Figure 3). The absorbance ratio was calculated considering the measured absorbance of the pure Mv 3-O-glc and pol-Anth solutions and taking into account the Mv 3-O-glc/pol (v/v) proportion used in each sample.

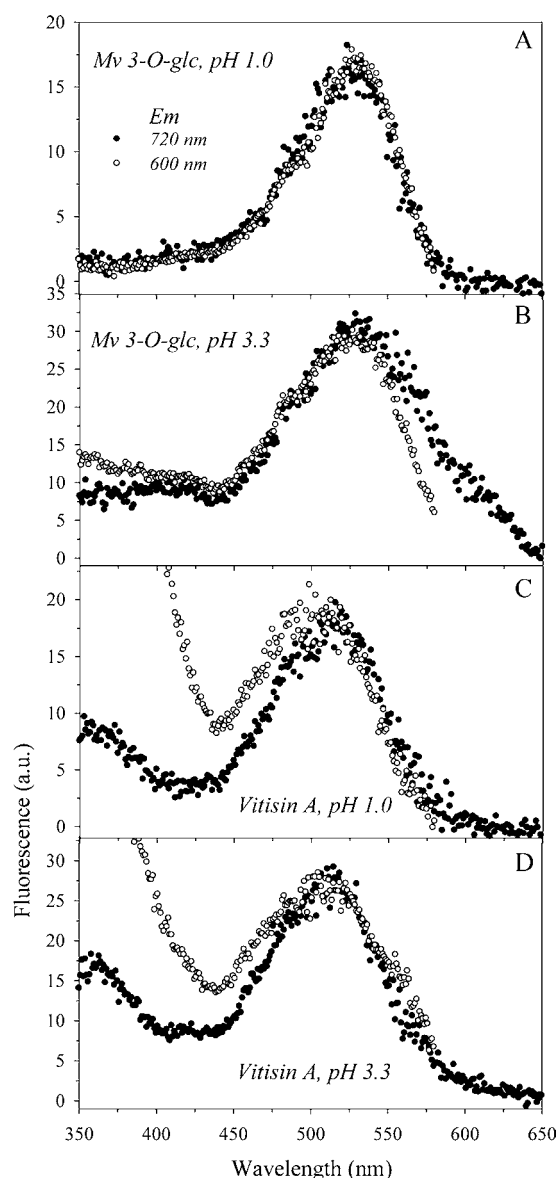


Figure 6. Fluorescence excitation spectra for emission at 720 nm (solid circles) and 600 nm (open circles) of malvidin 3-O-glucoside (Mv 3-O-glc) (A, B) and vitisin A (C, D) in aqueous/EtOH solutions at pH 1.0 (A, C) and pH 3.3 (B, D). Spectra with emission at 600 nm are normalized to the peak value of spectra with emission at 720 nm. Excitation spectra were corrected for differences in absorbance at 500 nm.

The relationship was found to fit well by an exponential function ($R^2 = 0.995$), although a linear regression could also be considered acceptable ($R^2 = 0.98$).

By measuring the F_{700}/F_{560} ratio on different wine samples and applying the above inverted exponential function, it was possible to estimate the mon-/pol-Anth absorbance ratio that is proportional to the relative content of the two classes of compounds. The results of this analysis are presented in Table 1.

From the results obtained and shown in Figures 2 and 3, older red wines are expected to have a lower F_{700}/F_{560} ratio and a consequent lower mon-/pol-Anth A ratio. As seen from Table 1, this was indeed observed for the two table wines tested and the four Port wines tested. Additionally, a young wine was analyzed directly as well as in the presence of sodium bisulfite

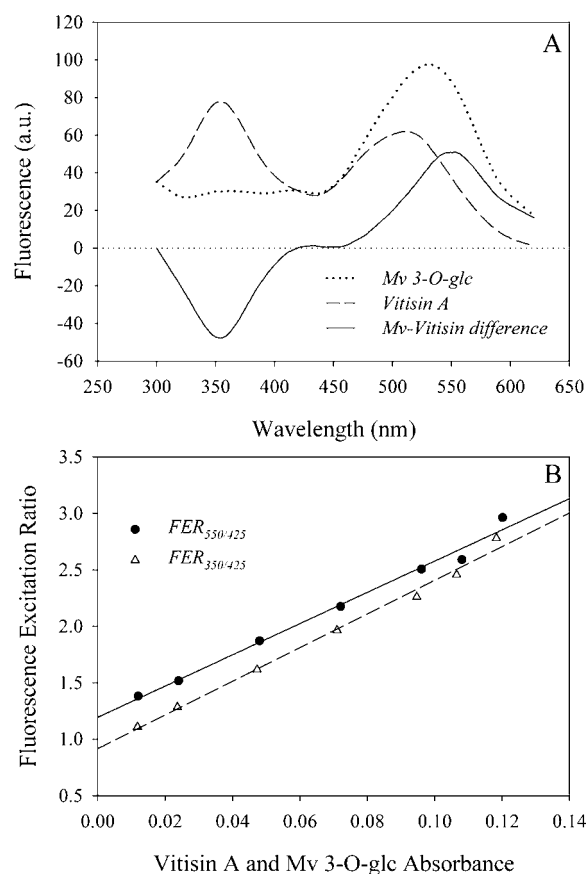


Figure 7. (A) Fluorescence excitation spectra of malvidin 3-O-glucoside (Mv 3-O-glc) and vitisin A in aqueous/EtOH solution at pH 3.3 for emission at 640 nm. Solid line represents the difference excitation spectrum between Mv and vitisin. (B) Fluorescence excitation ratios between 550 and 425 nm ($FER_{550/425}$) and between 350 and 425 nm ($FER_{350/425}$) as a function of absorbance of Mv 3-O-glc and vitisin A, respectively. R^2 of linear regressions > 0.995 .

or with polymerized anthocyanins. As expected, addition of sodium bisulfite or polymerized anthocyanins decreased the F_{700}/F_{560} and mon-/pol-Anth absorbance ratio. The addition of sodium bisulfite results in the bleaching of monomeric anthocyanins and hence a higher mon-/pol-Anth absorbance ratio.

Both monomeric and polymeric anthocyanins include several different kinds of pigments that are likely to present different fluorescence features. It becomes extremely difficult and complex to analyze all of these contributions as a whole.

Therefore, with the aim of better identifying the fluorescence contribution of the different classes of anthocyanin pigments present in red wine, more detailed assays were performed on two pigments representative of monomeric pigments: Mv 3-O-glc and vitisin A.

Spectroscopic Features of Mv-3-O-glc and Vitisin A.

Two representative of monomeric pigments, Mv 3-O-glc and vitisin A, were selected to study the fluorescence properties of anthocyanins and anthocyanin-pyruvic acid adducts. Malvidin 3-O-glucoside is the major anthocyanin detected in young red wine, and vitisin A is the main anthocyanin-derived pigment detected by HPLC after only 1 year of aging.¹¹

The UV-visible spectra of both pigments were first determined to compare them and to analyze the particular features arising from their different forms occurring in

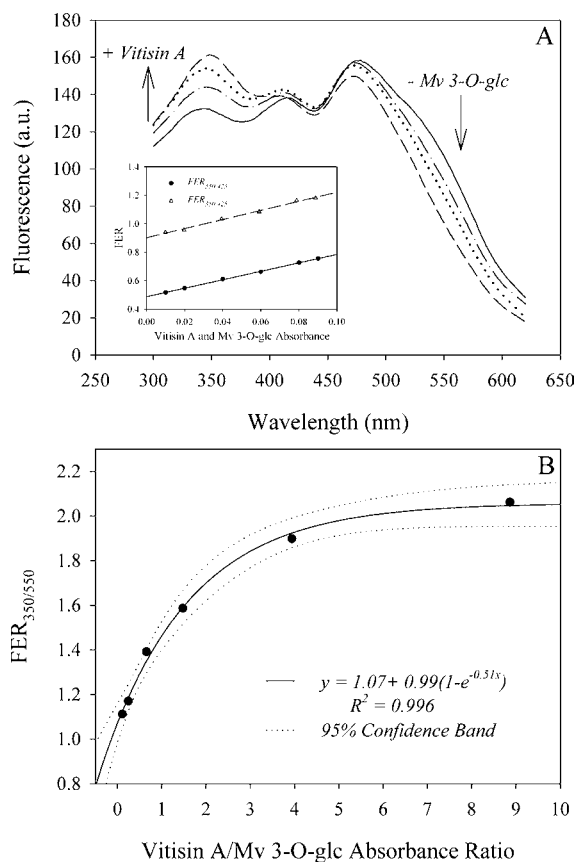


Figure 8. (A) Fluorescence excitation spectra of malvidin 3-O-glucoside (Mv 3-O-glc) and vitisin A in aqueous/EtOH solution at pH 3.3 for emission at 640 nm, with the presence of a fixed amount ($A = 0.033$) of pol-Anth. Volume/volume proportions of pure Mv and vitisin starting solutions were 9:1 (solid line), 6:4 (dash-dot line), 4:6 (dot line), and 1:9 (dash line). (Inset) Relationship between $FER_{350/425}$ and $FER_{350/550}$ as a function of Mv and vitisin absorbance, respectively. (B) Relationship between $FER_{350/550}$ and the vitisin A/Mv 3-O-glc absorbance ratio.

equilibrium. As already expected, the absorption spectrum of Mv 3-O-glc was significantly dependent on the pH of the solution. At pH 1.0, it showed a maximum absorption at 524 nm and shifted to 530 nm when the pH was raised to 3.3 (Figure 4). The enhanced absorption at longer wavelengths and the small hump around 600 nm at the less acidic conditions are likely due to the formation of the quinonoidal base. On the other hand, the large increase in absorbance below 400 nm may eventually be ascribed to the appearance of the hemiketal and chalcone forms. In contrast to Mv 3-O-glc, the absorption spectrum of vitisin A remained practically constant with the main band peaked at around 510 nm and a secondary band at 370 nm (Figure 4).

The fluorescence spectrum of Mv 3-O-glc at pH 1.0 showed a peak at 610 nm, which increased and shifted to 638 nm at pH 3.3. On the other hand, vitisin A showed a quite broad emission band with highest values around 720 nm at pH 1.0, whereas at pH 3.3 a significant increase in fluorescence was observed around 630 nm (Figure 5).

The fluorescence quantum yield of Mv 3-O-glc relative to vitisin A was found to be 1.24 and 1.16 at pH 1 and 3.3, respectively.

For both compounds and both pH values, a large Stokes shift (>100 nm) between absorption and emission band maxima was

observed. This is due to the presence of an efficient excited-state proton transfer (ESPT) from the excited flavylum cation to water, forming the excited quinonoidal base that emits at longer wavelengths.²⁹ Even at pH 1, where the flavylum cation is the only form present, the emission spectrum resulted from the overlapping of two emission bands, one at shorter wavelengths corresponding to the deactivation of the excited acid form and the other at longer wavelengths due to the relaxation of the excited base form. The increase in the fluorescence intensity, for both Mv 3-O-glc and vitisin A, from more to less acidic conditions can be explained by a pH-dependent proton quenching.³⁰

The presence of an excited-state deprotonation and emission from the resulting base was confirmed by comparison of the fluorescence excitation spectra recorded at 600 and 720 nm (Figure 6). For Mv 3-O-glc at pH 1 the two excitation spectra are properly overlapped (Figure 6A), meaning that both emissions come from the same form. These spectra were identical to the absorption spectrum of Mv 3-O-glc flavylum cation (see Figure 4), indicating that the fluorescence is due to the direct excitation of the flavylum form and the indirect production of the excited base by ESPT.

At pH 3.3, the excitation spectrum of Mv 3-O-glc for emission at 720 nm clearly deviates from that at 600 nm above 550 nm (Figure 6B). This means that a second fluorophore, besides the flavylum cation, contributes to the total fluorescence and that this contribution is likely due to the direct excitation of the quinonoidal base in the steady state. In fact, considering the pK_a (3.20) of the flavylum–quinonoidal base equilibrium,³¹ a significant concentration of the base is likely to be present at pH 3.3. On the other hand, the quinonoidal base possesses a significant absorption at 500 nm, thus contributing to the emission in the red under this excitation wavelength.^{15,29}

In the case of vitisin A, at both pH values (Figure 6C,D), a good agreement was observed between the excitation spectra at 600 and 720 nm around the peak and on the long wavelength side. This is consistent with the absence of large amounts of the quinonoidal base at pH quite below the pK_a (4.42).³² Below 480 nm, the higher values of excitation for the 600 nm emission compared to that of 720 nm probably derive from the tail of a large emission excited at around 350 nm (data not shown).

Fluorescence Approach To Distinguish Mv 3-O-glc from Vitisin A. From the difference excitation spectrum between Mv 3-O-glc and vitisin A for emission at 640 nm (Figure 7A), positive and negative maxima can be observed at about 550 and 350 nm, respectively, and almost nil values between 425 and 450 nm. Therefore, in a mixture of the two compounds, the fluorescence excitation ratio (FER) between wavelengths at the maximal difference and the isosbestic point can be used to follow changes in their concentration. The linear relationship between $FER_{550/425}$ and $FER_{350/425}$ and absorbance of Mv 3-O-glc and vitisin A, respectively, is shown in Figure 7B. These were obtained by combining two aqueous solutions of Mv 3-O-glc and vitisin A in different proportions and measuring the fluorescence excitation spectra of the mixtures. The absorbance of compounds was calculated considering the measured absorbance of the pure starting solutions and taking into account the Mv 3-O-glc/vitisin A (v/v) proportion used in each sample.

The above fluorescence excitation indices can be useful to follow the evolution of monomeric anthocyanins and their pyruvic acid adducts in wine fractions free of the polymeric

compounds. In whole wines, the strong contribution to fluorescence by the pol-Anth (as previously analyzed) makes it difficult to distinguish the two classes of pigments.

However, when a fixed aliquot of polymerized anthocyanins was added to the Mv 3-O-glc/vitisin A mixtures, the linear relationships between FER_{550/425} (FER_{350/425}) and Mv (vitisin) absorbance were maintained (see inset of Figure 8A). The differential changes of the excitation spectra as a function of the different proportions between Mv 3-O-glc and vitisin A were similar to those recorded in the absence of the pol-Anth (data not shown). Decreasing and increasing the Mv 3-O-glc and vitisin A contents produced a decrease of the 550 nm band and an increase of the 350 nm band, respectively (Figure 8A). FER_{350/550} can therefore be considered related to the absorbance ratio between vitisin A and Mv 3-O-glc, as reported in Figure 8B.

Conclusions. The present work constitutes the first attempt to use fluorescence to monitor the evolution of anthocyanin derivatives and to distinguish them from their anthocyanin precursors. This may allow not only the evolution of anthocyanin pigments to be monitored during wine aging but also the determination of age markers or even geographical markers.

Nevertheless, although promising, more wine samples will need to be tested to properly validate such methodology.

AUTHOR INFORMATION

Corresponding Author

*(N.M.) E-mail: nbmateus@fc.up.pt. Fax: +351.220402562. Phone: +351.220402659.

Funding

This research was supported by funding from FCT (), by a Project grant from FCT (Ação Integrada Luso-Italiana FCT/CNR), and by a postdoctoral grant from FCT (Fundação para a Ciência e a Tecnologia, Praxis BPD/65400/2009), all from Portugal, and by FEDER funding.

Notes

The authors declare no competing financial interest.

ACKNOWLEDGMENTS

We thank Eng. José M. Sousa Soares from Gran Cruz – Sociedade Comercial de Vinho, Lda for supplying the wines. This research was supported by a Project grant from both CNR and FCT (2011-2012 bilateral project), and a Post-doctoral grant from FCT (Fundação para a Ciência e a Tecnologia – Praxis BPD/65400/2009) from Portugal and by FEDER funding.

REFERENCES

- (1) Gómez-Plaza, E.; Gil-Muñoz, R.; López-Roca, J. M.; Martínez-Cutillas, A.; Fernández-Fernández, J. I. Phenolic compounds and color stability of red wines: effect of skin maceration time. *Am. J. Enol. Vitic.* **2001**, *52*, 266–270.
- (2) Liao, H.; Cai, Y.; Haslam, E. Polyphenol interactions. Anthocyanins: co-pigmentation and colour changes in red wines. *J. Sci. Food Agric.* **1992**, *59*, 299–305.
- (3) Remy-Tanneau, S.; Le Guerneve, C.; Meudec, E.; Cheynier, V. Characterization of a colorless anthocyanin-flavan-3-ol dimer containing both carbon-carbon and ether interflavanoid linkages by NMR and mass spectrometry. *J. Agric. Food Chem.* **2003**, *51*, 3592–3597.
- (4) Atanasova, V.; Fulcrand, H.; Le Guernevé, C.; Cheynier, V.; Moutounet, M. Structure of a new dimeric acetaldehyde malvidin 3-

glucoside condensation product. *Tetrahedron Lett.* **2002**, *43*, 6151–6153.

(5) Santos-Buelga, C.; Bravo-Haro, S.; Rivas-Gonzalo, J. C. Interactions between catechin and malvidin-3-monoglucoside in model solutions. *Z. Lebensm.-Unters.-Forsch.* **1995**, *201*, 269–274.

(6) Pissarra, J.; Lourenco, S.; Gonzalez-Paramas, A. M.; Mateus, N.; Buelga, C. S.; Silva, A. M. S.; De Freitas, V. Structural characterization of new malvidin 3-glucoside-catechin aryl/alkyl-linked pigments. *J. Agric. Food Chem.* **2004**, *52*, 5519–5526.

(7) Pissarra, J.; Mateus, N.; Rivas-Gonzalo, J.; Buelga, C. S.; de Freitas, V. Reaction between malvidin 3-glucoside and (+)-catechin in model solutions containing different aldehydes. *J. Food Sci.* **2003**, *68*, 476–481.

(8) Brouillard, R.; Chassaing, S.; Fougerousse, A. Why are grape/fresh wine anthocyanins so simple and why is it that red wine color lasts so long? *Phytochemistry* **2003**, *64*, 1179–1186.

(9) Fulcrand, H.; Atanasova, V.; Salas, E.; Cheynier, V. The fate of anthocyanins in wine: are there determining factors? In *Red Wine Color: Revealing the Mysteries*; Waterhouse, A. L., Kennedy, J. A., Eds.; American Chemical Society: Washington, DC, 2004; pp 68–88.

(10) Chassaing, S.; Lefeuvre, D.; Jacquet, R.; Jourdes, M.; Ducasse, L.; Galland, S.; Grelard, A.; Saucier, C.; Teissedre, P.-L.; Dangles, O.; Quideau, S. Physicochemical studies of new anthocyanin-ellagitannin hybrid pigments: about the origin of the influence of oak C-glycosidic ellagitannins on wine color. *Eur. J. Org. Chem.* **2010**, *2010*, 55–63.

(11) Mateus, N.; de Freitas, V. Evolution and stability of anthocyanin-derived pigments during port wine aging. *J. Agric. Food Chem.* **2001**, *49*, 5217–5222.

(12) Mateus, N.; Machado, J. M.; de Freitas, V. Development changes of anthocyanins in *Vitis vinifera* grapes grown in the Douro Valley and concentration in respective wines. *J. Sci. Food Agric.* **2002**, *82*, 1689–1695.

(13) Gomez-Alonso, S.; Garcia-Romero, E.; Hermosin-Gutierrez, I. HPLC analysis of diverse grape and wine phenolics using direct injection and multidetection by DAD and fluorescence. *J. Food Compos. Anal.* **2007**, *20*, 618–626.

(14) Cozzolino, D.; Kwiatkowski, M. J.; Parker, M.; Cynkar, W. U.; Damberg, R. G.; Gishen, M.; Herderich, M. J. Prediction of phenolic compounds in red wine fermentations by visible and near infrared spectroscopy. *Anal. Chim. Acta* **2004**, *513*, 73–80.

(15) Figueiredo, P.; Pina, F.; Vilasboas, L.; Macanita, A. L. Fluorescence spectra and decays of malvidin 3,5-diglucoside in aqueous solutions. *J. Photochem. Photobiol., A* **1990**, *52*, 411–424.

(16) Pina, F.; Melo, M. J.; Santos, H.; Lima, J. C.; Abreu, I.; Ballardini, R.; Maestri, M. Excited state proton transfer in synthetic flavylum salts: 4-methyl-7-hydroxyflavylium and 4',7-dihydroxyflavylium – example of a four-level molecular device to invert the population of the excited state. *New J. Chem.* **1998**, *22*, 1093–1098.

(17) Poustka, F.; Irani, N. G.; Feller, A.; Lu, Y.; Pourcel, L.; Frame, K.; Grotewold, E. A trafficking pathway for anthocyanins overlaps with the endoplasmic reticulum-to-vacuole protein-sorting route in *Arabidopsis* and contributes to the formation of vacuolar inclusions. *Plant Physiol.* **2007**, *145*, 1323–1335.

(18) Gomez, C.; Conejero, G.; Torregrosa, L.; Cheynier, V.; Terrier, N.; Ageorges, A. In vivo grapevine anthocyanin transport involves vesicle-mediated trafficking and the contribution of anthoMATE transporters and GST. *Plant J.* **2011**, *67*, 960–970.

(19) Wiltshire, E. J.; Collings, D. A. New dynamics in an old friend: dynamic tubular vacuoles radiate through the cortical cytoplasm of red onion epidermal cells. *Plant Cell Physiol.* **2009**, *50*, 1826–1839.

(20) Alimelli, A.; Filippini, D.; Paolesse, R.; Moretti, S.; Ciolfi, G.; D'Amico, A.; Lundstrom, I.; Di Natale, C. Direct quantitative evaluation of complex substances using computer screen photo-assisted technology: the case of red wine. *Anal. Chim. Acta* **2007**, *597*, 103–112.

(21) Azevedo, J.; Teixeira, N.; Oliveira, J.; de Freitas, V.; Mateus, N. Effect of sugar acylation on the antioxidant properties of *Vitis vinifera* red grape malvidin-3-glucoside. *Int. J. Food Sci. Technol.* **2011**, *46*, 343–349.

(22) Oliveira, J.; Fernandes, V.; Miranda, C.; Santos-Buelga, C.; Silva, A.; de Freitas, V.; Mateus, N. Color properties of four cyanidin-pyruvic acid adducts. *J. Agric. Food Chem.* **2006**, *54*, 6894–6903.

(23) Oliveira, J.; Azevedo, J.; Silva, A. M. S.; Teixeira, N.; Cruz, L.; Mateus, N.; de Freitas, V. Pyranoanthocyanin dimers: a new family of turquoise blue anthocyanin-derived pigments found in Port wine. *J. Agric. Food Chem.* **2010**, *58*, 5154–5159.

(24) Oliveira, J.; Silva, M. A. d.; Jorge Parola, A.; Mateus, N.; Brás, N. F.; Ramos, M. J.; Freitas, V. d. Structural characterization of a A-type linked trimeric anthocyanin derived pigment occurring in a young Port wine. *Food Chem.* **2013**, *141*, 1987–1996.

(25) Somers, T. C. The polymeric nature of wine pigments. *Phytochemistry* **1971**, *10*, 2175–2186.

(26) Esti, M.; Venanzi, M. In *Detection and characterization of the photophysical properties of anthocyanins in wine by fluorescence techniques and flash photolysis measurements*, International Conference on Polyphenols; Finland, 2004; Hoikkala, A., Wähälä, K., Eds.; Gummerus Printing: Helsinki, Finland, 2004.

(27) Berké, B.; Chèze, C.; Deffieux, G.; Vercauteren, J. Sulfur dioxide decolorization or resistance of anthocyanins: NMR structural elucidation of bisulfite-adducts. In *Plant Polyphenols 2*; Gross, G.; Hemingway, R., Yoshida, T., Branham, S., Eds.; Springer: New York, 2000; Vol. 66, pp 779–790.

(28) Bakker, J.; Preston, N. W.; Timberlake, C. F. The determination of anthocyanins in aging red wines: comparison of HPLC and spectral methods. *Am. J. Enol. Vitic.* **1986**, *37*, 121–126.

(29) Moreira, P. F.; Giestas, L.; Yihwa, C.; Vautier-Giongo, C.; Quina, F. H.; Macanita, A. L.; Lima, J. C. Ground- and excited-state proton transfer in anthocyanins: From weak acids to superphotoacids. *J. Phys. Chem. A* **2003**, *107*, 4203–4210.

(30) Harris, C. M.; Selinger, B. K. Proton-induced fluorescence quenching of 2-naphthol. *J. Phys. Chem.* **1980**, *84*, 891–898.

(31) Houbiers, C.; Lima, J. C.; Macanita, A. L.; Santos, H. Color stabilization of malvidin 3-glucoside: self-aggregation of the flavylium cation and copigmentation with the Z-chalcone form. *J. Phys. Chem. B* **1998**, *102*, 3578–3585.

(32) Oliveira, J.; Mateus, N.; de Freitas, V. Network of carboxypyranomalvidin-3-O-glucoside (vitisin A) equilibrium forms in aqueous solution. *Tetrahedron Lett.* **2013**, *54*, 5106–5110.